

ELECTRON MIGRATION AND STABILITY OF DYE SOLAR CELLS

L. le Roux*¹, S. Hietkamp²

^{1,2}CSIR - Materials Science and Manufacturing, PO Box 395, Pretoria 0001, South Africa, www.csir.co.za

Abstract

Dye-sensitised photoelectrochemical solar cells with four different electrolyte combinations were assembled and characterised using current–voltage measurements. The effects that the solvents (acetonitrile - ACN and propionitrile - PN) have on the efficiency of the cells were investigated. Two physical properties of the solvents (viscosity and permittivity) were used in this comparison.

Electrochemical impedance spectroscopy (Nyquist and Bode plots) was used for analysis of the charge transfer processes.

The different electrolyte combinations had a significant difference on the short circuit currents (I_{SC}) 42 and 48 mA for B and A respectively while the solvents had almost no effect. The results show that the solvents have the greatest effect on the efficiencies of the cells.

Keywords

Dye Solar Cell, Nyquist plot, Bode plot, I–V curve; Impedance spectroscopy, viscosity, permittivity

Contents

1. Introduction

2. Experimental

2.1 Efficiency measurements

2.2 Impedance measurements

3. Results and Discussion

3.1 Average efficiencies of the four different electrolyte combinations

3.2 Efficiency and impedance

3.3 The effect of solvent viscosity on the efficiency

3.4 The effect of *permittivity* (dielectric constant) on the cell efficiency.

4. Conclusions

5. Acknowledgements

6. References

1. Introduction

According to Hoshikawa *et al.* [1] the three major components (areas) of charge transfer in dye solar cells are TiO₂/electrolyte (working electrode) diffusion of the I₃⁻ ions in the electrolyte and the Pt/electrolyte (counter electrode). According to literature [2], the use of additives such as TBP (tertiary butyl pyridine) and MBI (methyl benzimidazole) would improve the output voltage of the cell. Nazeeruddin *et al.* [2] determined that the TBP causes an increase in the energy of the Fermi level due to a decrease in electron recombination from the TiO₂ surface to the I₃⁻. In a study that was done by Shi *et al.*, [3] they concluded that TBP can also remove iodine that is adsorbed on the dye which will lead to suppress the rate of interfacial electron transfer from the conduction band of TiO₂ to iodine. The electrolyte which contained the TBP showed a slightly higher efficiency than the electrolyte with the MBI, which confirms the work that was reported by Boschloo [4] and Xiong [5]. Sommeling *et al.* [6] determined that due to the large excess iodine in the electrolyte (0.05 and 0.1 M), the effect of depletion could not be observed in either of the electrolytes. In this paper we investigated the use of impedance spectroscopy to explain the difference in efficiencies with reference to the viscosity and permittivity of the solvents. Dye-sensitised photoelectrochemical solar cells (DSCs) with four different electrolyte combinations were assembled. The effects of the solvents (acetonitrile and propionitrile) as well as the effects that the electrolytes have on the efficiency of the cells were compared. Solvent properties such as viscosity and permittivity were compared.

2. Experimental

Master plates were assembled in the laboratories at ECN in the Netherlands. Each plate consisted of five identical cells of 0.8 cm x 5.0 cm (4.0 cm²). Figure 1 is an example of a master plate that was used for this work. The TiO₂ was screen printed on the working electrode as well as the Pt for the counter electrode. After annealing at 450 °C the cells were sealed by using two layers of Surlyn 1702 (hot wax) and a vacuum laminator. The dye was deposited by pumping a $\sim 3 \times 10^{-4}$ M solution in alcohol through the cells at 80 °C for 20 minutes. After the deposition of the dye, the electrolyte was introduced and the holes were sealed. The composition of the electrolyte solutions are detailed in Table 1. Each of the two electrolyte combinations were dissolved in acetonitrile (ACN) and propionitrile (PN) to give the four different combinations (A ACN, A PN, B ACN and B PN). Each electrolyte combination was used in five cells to ensure reproducibility.

2.1 Efficiency measurements

The performance of the cells was evaluated by generating I/V curves with a MTSP (Mobile Testing Station for Photovoltaics purchased from Dyesol, Australia) which allowed the calculation of the cell efficiencies. The scanning voltage range was -0.1V to 0.8V and was plotted from 0V to 0.8V. The light source was a Solar Simulator purchased from “Sciencetech” in the USA. All efficiency measurements were done under illumination of 100 mW/cm² (one sun).

2.2 Impedance measurements

The impedance spectra of the cells were generated over a frequency range of 10⁻¹ to 10⁶ Hz with the AC amplitude set at 10 mV using a frequency response analyzer

(Autolab PGSTAT 12/30/230). The illumination intensity was one sun and no bias voltage was applied during these measurements.

Figure 2 presents the different zones (arcs) in the Nyquist plot. $R_1 + R_h + R_3$ approximate the series resistance (R_s) of the cell [7]. R_h is equivalent to the sheet resistance of the substrate. Therefore higher resistance values are indicative of lower efficiencies.

The charge transfer resistance (R_{CT}) is the sum of the impedance of Z_1 , Z_2 and Z_3 . The charge transfer resistance (R_{ct}) as well as the series resistance (R_s) can also be obtained from the bode plots [8], [9] (fig. 7). R_2 is equivalent to the resistance of a diode Z_2 and is mainly a result of the recombination reaction of TiO_2 electrons [7].

3. Results and Discussion

Table 1: Detail of the two different electrolyte formulations

A		B	
HMMI	0.6 M	DMPH	0.6 M
LiI	0.1 M	MBI	0.5 M
I ₂	0.05 M	I ₂	0.1 M
TBP	0.5 M		

where:

HMMI: hexylmethylimidazolium iodide; TBP: 4-tertiary butyl pyridine; DMPH: dimethylpropyl imidazolium iodide; MBI: N-methylbenzimidazole

3.1 Average efficiencies of the four different electrolyte combinations

In table 2 it is shown that the ACN cells have higher efficiencies than the PN cells.

Electrolyte A, which contains TBP, showed slightly higher efficiencies than B that does not contain any TBP but MBI. The slight increase in efficiency is due to the addition of TBP which was confirmed in a study by Zang *et al.*[10].

Table 2: Summary of the results for the efficiency measurements

Cell name	I_{sc} (mA)	V_{oc} (volts)	ff	η (%)
B PN	48	0.72	0.44	3.9 ± 0.1
B ACN	48	0.70	0.56	4.6 ± 0.2
A PN	41	0.76	0.51	3.9 ± 0.2
A ACN	41	0.76	0.51	5.1 ± 0.1

The average I/V curves for the different electrolyte combinations are shown in Figure 3.

The different electrolytes give different I_{sc} (short circuit current) values. The different solvents do not have a significant effect on the I_{sc} . Electrolyte B gives a higher short circuit current (48 mA) than electrolyte A (41 mA) but recombination reactions start to occur at lower voltages (0.2V for PN and 0.3V for ACN). For electrolyte A, recombination reactions start at 0.35V and 0.5V respectively for PN and ACN.

According to Hoshikawa *et al.* [11], the plateau of each I–V curve corresponds to the diffusion-limiting current (I_0). The difference between the short circuit current, I_{sc} , and the measured current, I , is the diffusion-limiting current, I_0 . Considering the plateau of the

I/V curve where, $I_0 = 0$ and $I = I_{sc}$, which is in agreement with the adapted diode equation for dye solar cells (eq.1).

$$I = I_0[\exp(qV/nkT) - 1] + I_{sc} \quad (1)$$

(diode equation adapted for DSC)[12]

where:

I = net current flowing through the cell; q = the charge of an electron (1.602×10^{-19} C); k = Boltzmann's constant (1.38×10^{-23} JK⁻¹); I_0 = diode saturation current (the larger I_0 , the larger the recombination); T = absolute temperature (K); n = the diode ideality factor ($1 < n < 2$ and increases if the current decreases).

3.2 Efficiency and impedance

The impedance of the cells with ACN as solvent, (highest efficiencies) was significantly smaller than the impedance values for the cells with PN as solvent. Figure 4 shows the impedance spectra (Nyquist plots) for the four different cells. The cells with ACN as solvent show three distinct arcs while the cells with PN as solvent, only show one arc. It is likely that the arc due to the TiO₂/dye/electrolyte interface charge transfer processes (middle arc in figure 4 or Z_2 in figure 2) is enlarged to such an extent that the small arcs (Z_1 and Z_3) became hidden (overlapped). The expansion of the radial frequency (ω in figure 4) for PN suggests that there is less electron injection from the dye which leads to a smaller the electron concentration in TiO₂, and therefore the number of electrons transferring at TiO₂|electrolyte is less if compared with ACN. The characteristic radial frequency of the Z_2 arc (fig 4.) in the Nyquist plot is lower for ACN than for PN (400 vs. 4000). This frequency is also known as the inverse of recombination lifetime (electron lifetime) of an electron in the TiO₂ layer [11]. The two Nyquist plots for the electrolytes

with ACN as solvent are about the same size (fig. 4), which is an indication that they both have about the same number of electrons to transfer between the electrolyte and TiO₂ [11]. The arc with the lower radial frequency (ACN) indicates slower recombination and therefore a higher efficiency (see table 2).

According to the Bode phase plots (fig. 5, 6 and 7), it can be seen that PN has a significantly larger phase shift value than ACN. This is consistent with the theory that there is a decrease in the electron recombination time - faster reverse reactions - [13] which would lead to lower efficiencies. This implies that the photovoltage decreases because of a decreasing electron lifetime. This is also consistent with the efficiency measurements that show that the cells that contain ACN has higher efficiencies than PN containing cells.

Table 3: Physical properties of ACN and PN

Solvent Physical properties	ACN	PN
Molecular mass (g/mole)	41	55
Melting point (°C)	-46	-92
Boiling point (°C)	80	97
Vapour density (air = 1)	1.41	1.9
Vapour pressure (mm Hg at 20°C)	72.8	39
Viscosity (cP at 25°C)	0.343	0.411
Permittivity at 20°C	37.2	27.2
Specific gravity (g/cm ³ at 25°C)	0.777	0.7818
Flash point (°C)	6	6

3.3 The effect of solvent viscosity on the efficiency

Diffusion coefficients increase with increasing temperature according to the Stokes-Einstein equation but, in this study, the temperatures were kept constant so it was not studied. The viscosities of the two solutions differ at the same temperature. For the diffusion of spherical molecules or particles in a solvent, the Stokes-Einstein relation is valid, that is, the diffusion coefficient (D) is equal to:

$$D = kT/(6 \pi \eta r) \quad (2)$$

where, η is the kinematic viscosity, and r is the radius of the diffusing species [14].

Equation (2) shows that an increase in viscosity will result in a decrease in the diffusion coefficient. This relates to lower cell efficiencies as shown in Table 2. The difference in D for the two solvents was calculated from data in table 3 to be more than 16%. The difference in efficiency (Table 2) is 23 %.

Dloczik showed that the fitting of the phase angle plot is particularly sensitive to the electron lifetime and diffusion coefficient [15]. The higher viscosity of PN also contributes to a lower charge transfer rate (higher impedance values).

The diffusion behaviour of the electrolyte will also affect the back reaction and electron transport in the DSC that will result in an increase in the impedance [16]. The effect of the viscosity of the solvent can be seen in the difference in the impedance spectra and the performance of the DSC (see figures 1 and 3). For the electrolyte with PN as solvent it appears that the arc due to the recombination (middle arc in figure 4 or Z_2 in figure 2) is enlarged to such an extent that the small arcs became hidden (overlapped).

The radii of the ionic species in electrolyte A were the same but this does not necessarily relate to equal size of the solvated species due to the different solvents.

3.4 The effect of permittivity on the cell efficiency.

The permittivity of ACN is larger than that for PN (37.2 vs. 27.2). The permittivity is directly related to electric susceptibility. For example, in a capacitor, an increased permittivity allows the same charge to be stored with a smaller electric field (and thus a smaller voltage), leading to an *increased capacitance*. As the capacitance is increased (ac voltage), a larger number of electrons change plates every cycle and therefore the current is increased. The following equations will show the relationship between the permittivity and impedance.

$$C = \varepsilon A/d \quad (3)$$

(C = capacitance, ε = permittivity, A = area of each plate and d = distance between the plates)

and

$$C = V/I = -j/2 \pi f Z \quad (4)$$

Z = Impedance, V = voltage, I = current, j = imaginary unit, f = frequency

Therefore

$$\varepsilon A/d = -j/2 \pi f Z \quad (5)$$

$$Z = -jd/2 \pi f \varepsilon A \quad (6)$$

An increase in permittivity (increase in capacitance) will result in lower impedance which is shown in figure 4.

4. Conclusions

- In this case the effect of the *solvent* is the major contributor to the difference in cell efficiencies.
- The Nyquist plot as well as the Bode plot can give an indication of the relative efficiencies. The higher the value for the phase shift, the lower the efficiency.
- The solvent with the higher permittivity (ACN) contributes to a higher efficiency through higher capacitance.
- The solvent does not have an effect on the I_{sc} while the different electrolyte combinations have an effect on the I_{sc} .

5. Acknowledgements

CSIR – Sponsors of the project

6. References

- [1] T. Hoshikawa, M. Yamada, R. Kikuchi and K. Eguchi. *Journal of Electroanalytical Chemistry* **577** (2005), p. 339-348.
- [2] M.K. Nazeeruddin, A. Kay and I.J. Rodicio. *J. Am. Chem. Soc.* **115** (1993), p. 6382-6390.
- [3] Shi, C., Dai, S., Wang, K., Pan, X., Kong, F. and Hu, L. *Vibrational Spectroscopy* **39** (2005), p. 99–105.
- [4] G. Boschloo, L. Häggman, and A. Hagfeldt, *J. Phys. Chem. B* **110** (2006), p. 13144-13150.
- [5] B. Xiong, B. Zhou, Z. Zhu, T. Gao, L. Li, J. Cai and W. Cai, *Chinese Journal of Chemistry* **26** (2008), p. 70-76.

- [6] P. M. Sommeling, M. Späth, H. J. P. Smit, N. J. Bakker and J. M. Kroon. *Journal of Photochemistry and Photobiology A: Chemistry*. **164** (2004), p. 137-144.
- [7] L. Han, N. Kiode, Y. Chiba, A. Islam and T. Mitate, *C.R. Chimie* **9** (2006) p. 645-651.
- [8] A. Hauch & A. Georg, *Electrochim. Acta* **46** (2001), p. 3457-3466
- [9] J. M. Kroon, N. J. Bakker, H. J. P. Smit, P. Liska, K. R. Thampi, P. Wang, S. M. Zakeeruddin, M. Grätzel, A. Hinsch, S. Hore, U. Würfel, R. Sastrawan, J. R. Durrant, E. Palomares, H. Pettersson, T. Gruszecki, J. Walter, K. Skupien and G. E. Tulloch. *Prog. Photovolt: Res. Appl.* **15** (2007) p. 1–18
- [10] C. Zhang, J. Dai, Z. Huo, X. Pan, L. Hu, F. Kong, Y. Huang, Y. Sui, X. Fang, K. Wang, and S. Dai. *Electrochim. Acta* **53** (2008), p. 5503-5508.
- [11] T. Hoshikawa, T. Ikebe, R. Kikuchi, and K. Eguchi. *Electrochim. Acta* **51** (2006), p. 5286-5294.
- [12] A. Zaban, J. Zhang, Y. Diamant, O. Melemed, and J.J. Bisquert. *Phys. Chem. B* **107** (2003), p. 6022-6025.
- [13] A.C. Fisher, L.M. Peter, E.A. Ponomarev, A.B. Walker and K.G.U. Wijayantha. *J. Phys. Chem. B* **104** (2000), p. 949-958.
- [14] J.E. Evanoff and W.D. Harris. *Can. J. Chem.* **56** (1978), p.574.
- [15] L. Dloczik, O. Ileperuma, I. Laueremann, L.M. Peter, E.A. Ponomarev, G. Redmond, N.J. Shaw and I. Uhlendorf, *J. Phys. Chem. B* **101** (1997), p. 10281 - 10289.
- [16] J. Jiu, F. Wang, M. Sakamoto, J. Takao and M. Adachi. *Solar Energy Materials and Solar Cells* **87** (2005), p. 77-86.

Figures

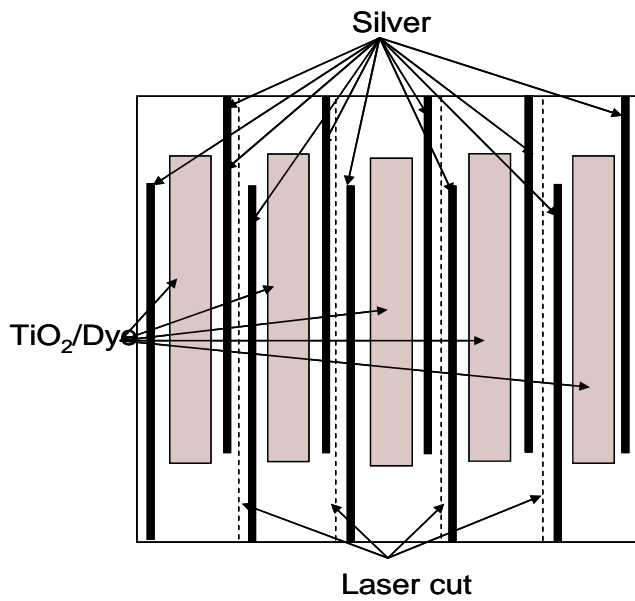


Figure 1: The design of a master plate that was used for the experiments

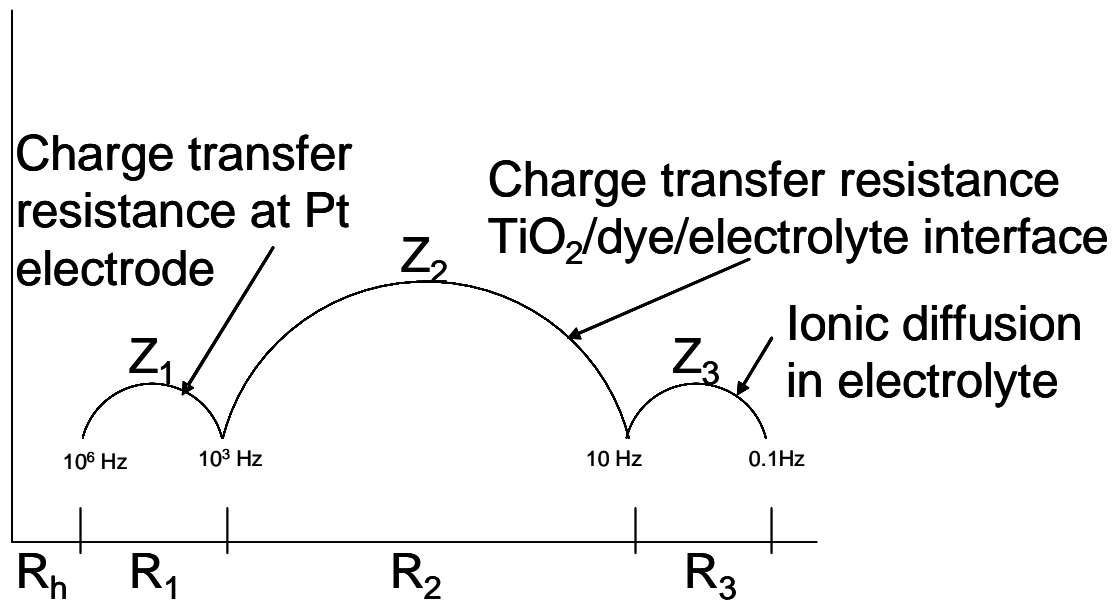


Figure 2: Different zones of the Nyquist plot for DSCs. The frequency ranges are typical that would be found during potentiometric analysis.

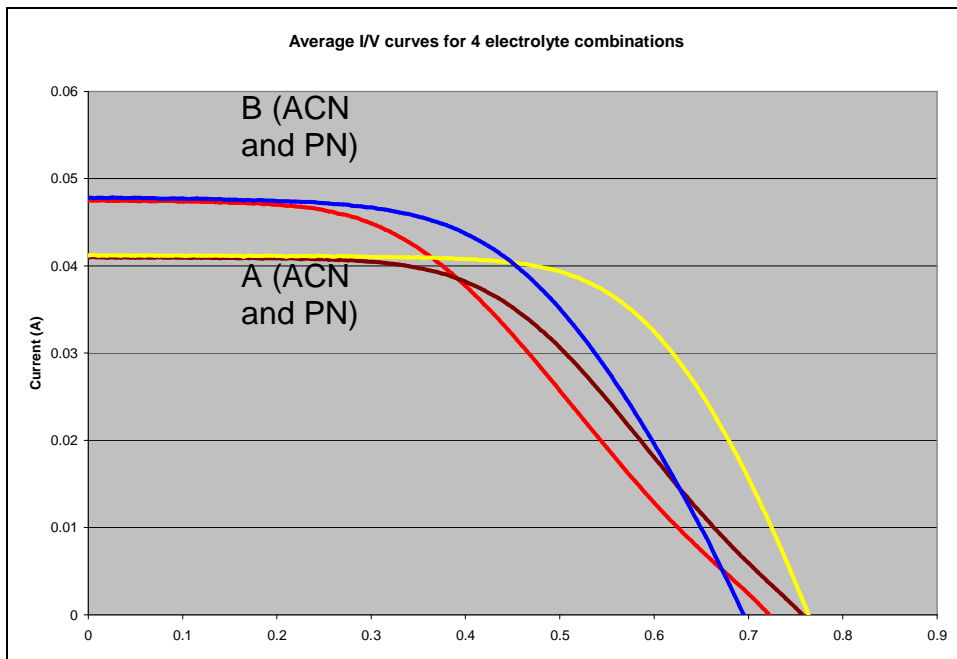


Figure 3: Average I/V curves for the different electrolyte combinations. Note the short circuit currents for the different electrolytes are the same. (Blue – ACN, Red – PN, Yellow – ACN and Brown – PN)

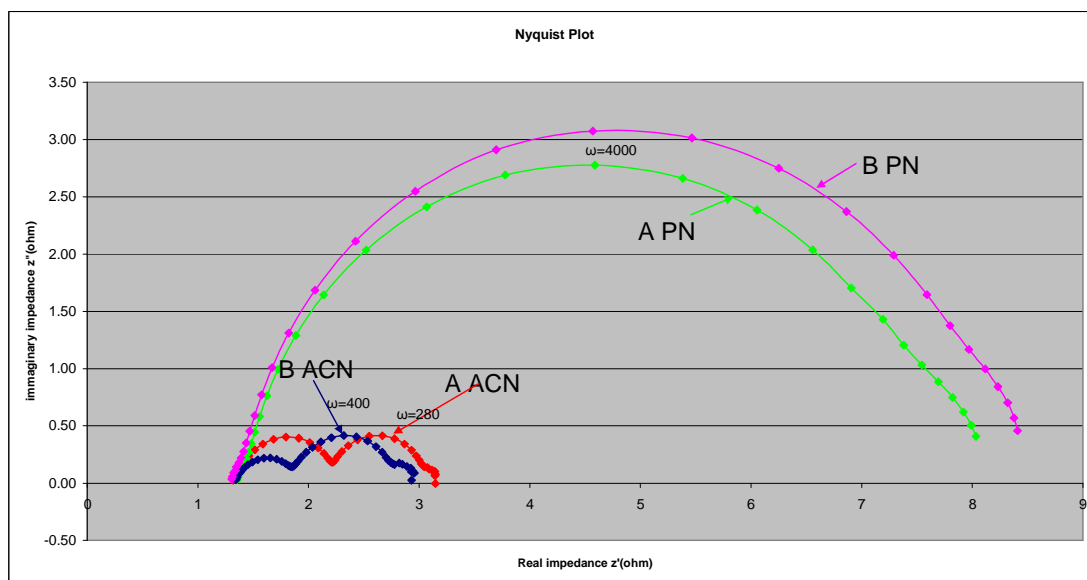


Figure 4: Nyquist plot of the four different cell combinations under illumination of 1 sun and 0V bias potential. (Blue and Red – ACN; Pink and Green – PN). ω = radial frequency.

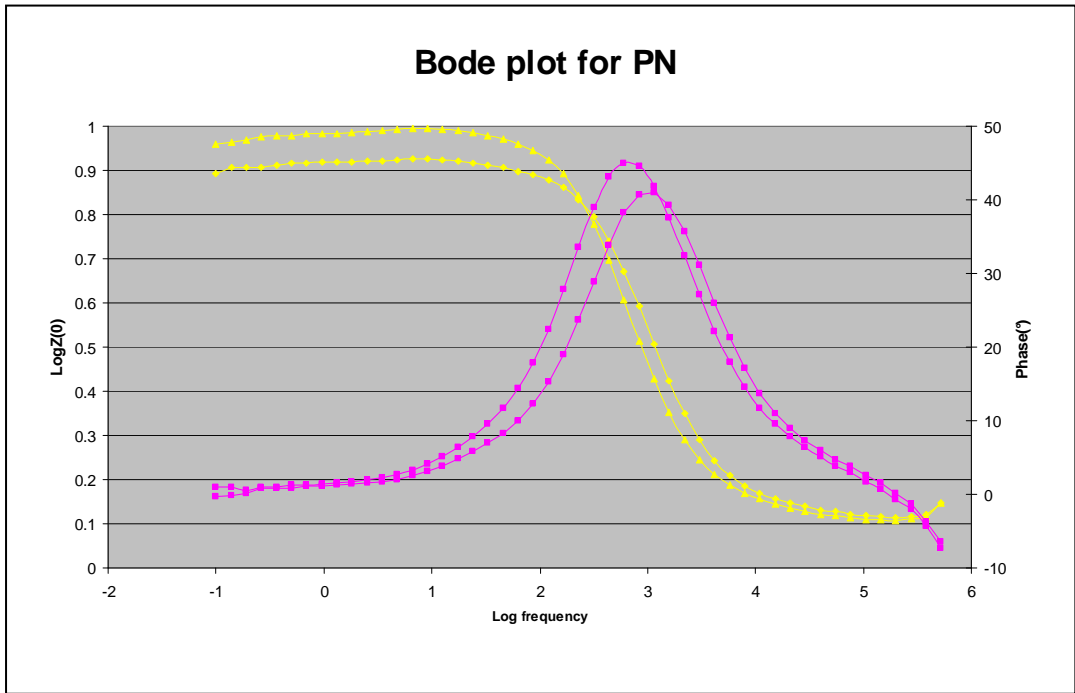


Figure 5: Bode phase plots of electrolytes A and B in propionitrile under illumination of 1 sun and 0V. Yellow graphs indicate the $| \text{impedance} |$ and the pink the phase plots.

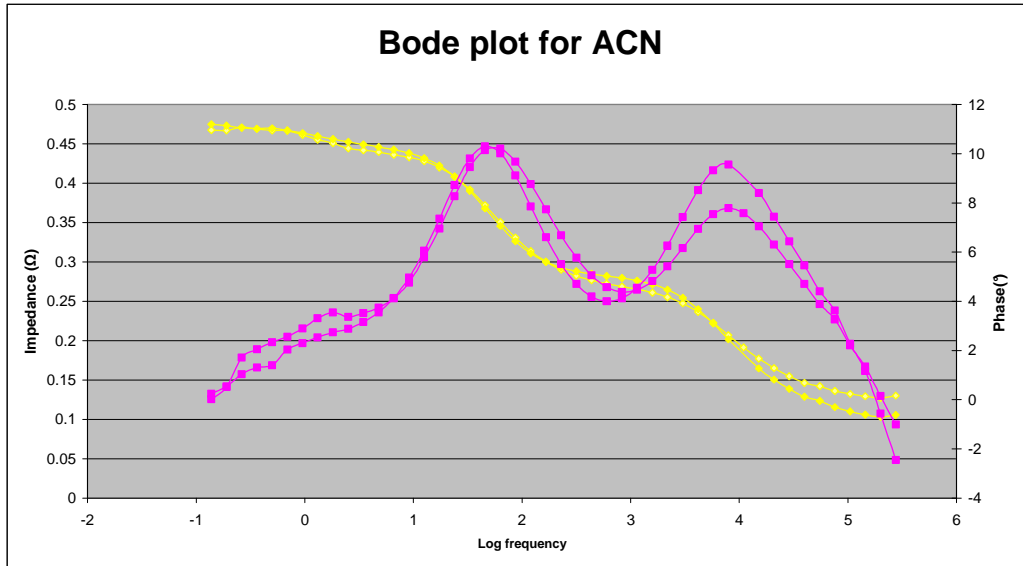


Figure 6: Bode plots of electrolytes A and B in acetonitrile under illumination of 1 sun and 0V. Yellow graphs indicate the $| \text{impedance} |$ and the pink the phase plots.

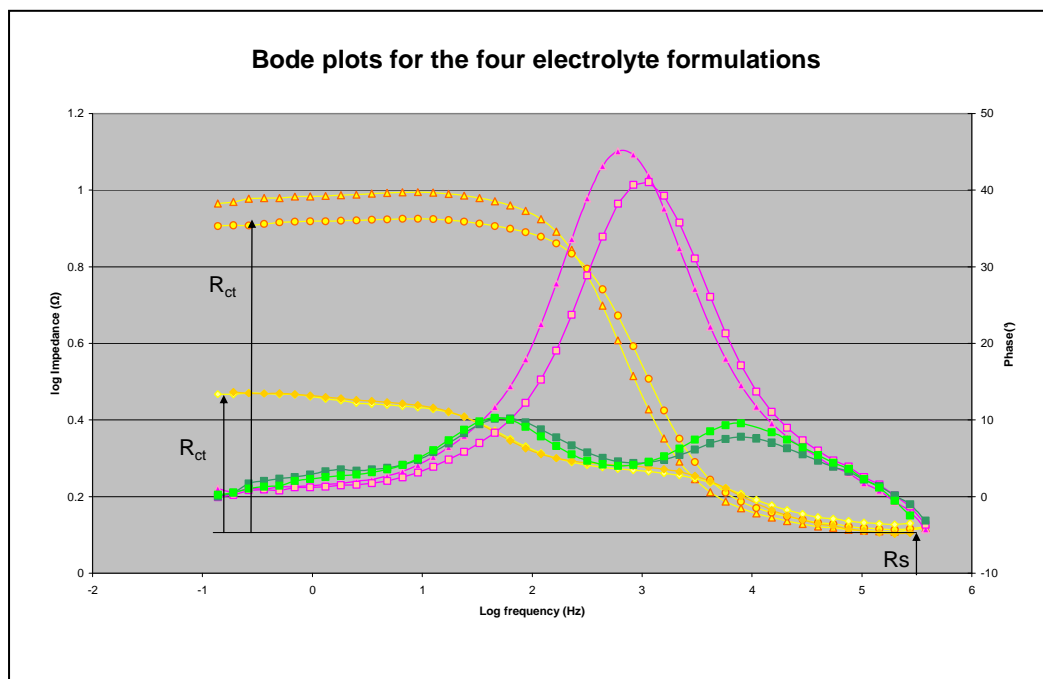


Figure 7: Bode plots of all four electrolyte combinations under illumination of 1 sun and 0V. Note that the charge transfer resistance R_{ct} and the series resistance of the cell R_s .